

On the Unified Theory of Atmospheric Particle Systems Part II: Self-affine Particles

Liu Yangang (刘延刚)

Desert Research Institute, Atmospheric Sciences Center, Reno, NV 89506, USA

Received May 13, 1996; revised January 2, 1997

ABSTRACT

As the second attempt at unifying treatment of atmospheric particle systems, this paper further examines shape characterization of atmospheric particles. First, to support the theoretical framework developed in Part I, methods for studying non-spherical particles are reviewed. It is argued that these different methods can be unified under fractal geometry through the generalized power laws given in Part I. Empirical power-laws for hydrometeors scattered in literature since 1935 are summarized and reevaluated in terms of fractals. Second, generalization from self-similar to self-affine particles is discussed. Self-affinity of atmospheric particles is exemplified by examining the exponents in the power laws between the length along a - and c -axis of ice crystals. It is argued that unlike Euclidean and self-similar particles, self-affine particles do not have a simple dimensional relation between original particles and their projections; the relation for projection of self-similar particles and Mandelbrot' thumb rules for intersection respectively set the lower and upper bound. Using published data, self-affine particles are shown to exist in the atmosphere. The existence of self-affine particles in turn calls for instruments that can simultaneously measure mass, area and maximum diameter (or their equivalents).

Key words: Atmospheric particle, Shape quantification, Power-law, Self-affine fractal, Instrumentation

I. INTRODUCTION

Atmospheric particles include both aerosols and hydrometeors. Traditionally, they are studied separately. However, many atmosphere-related problems such as global climate call for an overall consideration of effects from all the atmospheric particles. Moreover, since these particles interact with one another, it is desirable to describe atmospheric particle systems as a whole. Theory of atmospheric particle systems has two relevant problems that are not completely understood: particle shape and number distribution. Liu (1995, hereafter Part I) addressed both issues within a unified framework, in which particle shapes are unified with fractal geometry, particle number size distributions are unified with the principle of maximum Shannon's entropy, and particle shapes are related to particle number size distribution through shape-dependent power-laws.

With three specific objectives, this paper further examines shapes of atmospheric particles and their characterization. First, Part I only discussed particle shapes theoretically. How to treat non-spherical particles has been explored for a long time. Aerosol scientists and meteorologists treat non-sphericity differently. To provide observational evidence for the potential of unifying shape treatment through the generalized power laws developed in Part I, previous studies will be reviewed, summarized and re-considered in terms of fractals. Second, Part I concentrated on Euclidean and self-similar particles. However, particles of neither Euclidean nor self-similar shapes also exist in the atmosphere. A unified scheme therefore should have the ability to quantify more general shapes. The second objective is to extend

particle shapes from self-similar to self-affine fractals, to demonstrate the existence of self-affine particles in the atmosphere. To discuss what new questions the existence of self-affine particles poses for future research is the third goal.

The paper is organized as follows. Section 2 reviews approaches used by aerosol scientists and meteorologists to investigate non-spherical particles, and summarizes applications of fractal geometry in investigations of aerosol, and empirical power laws for hydrometeors. In Section 3, first discussed are dimension concepts and methods for determining fractal dimensions, then self-similar and self-affine fractals with emphasis on their distinctions. In Section 4, two methods for studying self-affine particles are discussed, and applied to demonstrate the existence of self-affine particles in the atmosphere. The existence of self-affine particles complicates shape quantification and hence raises new requests for instrumentation. These implications are discussed in Section 5. Concluding remarks are made in Section 6.

II. OVERVIEWS AND RE-EVALUATION

Non-spherical particles have been studied for a long time in many disciplines. However, how to treat non-sphericity remains unsolved. Approaches for aerosols and hydrometeors are different. As noted in Part I, a unified treatment is necessary for studying problems related to atmospheric particles. This section serves to review, summarize and re-evaluate methods for treating non-spherical particles, and show these different methods can be unified under fractal geometry through the generalized power laws given in Part I.

1. Studies of Non-spherical Aerosols

For a non-spherical particle, a commonly used term in aerosol science is equivalent

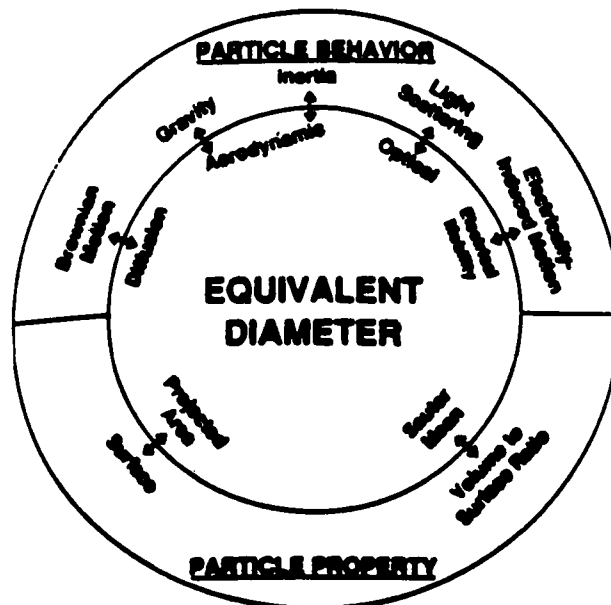


Fig. 1. Various equivalent diameters and corresponding physical quantities measured (After Baron and Willeke, 1993).

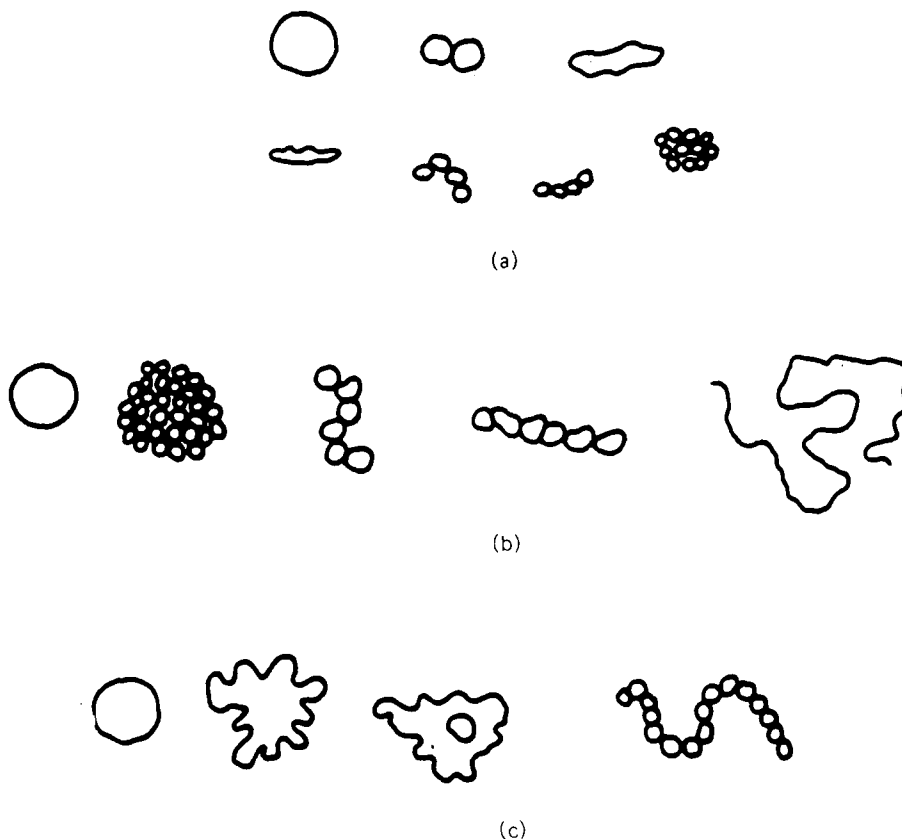


Fig. 2. Particles that look different can belong to the same set when described by a descriptor: (a) set of particles that have the same “projected area diameter”; (b) set of particles of identical Stokes diameter; (c) set of particles with same volume. (after Kaye 1981, Fig.1.2).

diameter. When a particle is detected by a technique, the measurement usually corresponds to a specific physical property. An equivalent diameter is then defined as the diameter of a sphere having the same value of a specific physical property as the non-spherically shaped particle being measured. For instance, aerodynamic equivalent diameter is the diameter of a unit-density sphere having the same gravitational settling velocity as the particle being measured. The commonly used equivalent diameters and corresponding properties are summarized in Fig.1. Such equivalent diameter method has the deficiency that it can hardly differentiate between distinct shapes. Fig.2 provides good examples: particles with very different shapes may have the same equivalent diameters.

The deficiency of “equivalent diameter” method is partially overcome by adding a shape factor (Herdan et al. 1960, 25–27pp; 173–180pp). Theory for non-spherical particles hence involves a shape factor and an equivalent diameter. For example, drag on a non-spherical particle is often expressed as a function of dynamic shape factor and volume equivalent diameter. However, such “shape factor approach” is unsatisfactory since most shape factors are empirically determined by comparing two different measurements, and therefore are of uncertainty.

Thanks to the application of fractal geometry, a major breakthrough occurs in aerosol

shape characterization (Kaye 1978; see also the references listed in Tables 2a and 2b). Three ways have been developed to determine fractal dimension. The standard one, ruler method, is to determine fractal dimension by measuring some property (e.g., number of sphere $N(L)$) change with the scale of the ruler (e.g., a length L) for an individual particle. The fractal dimension is determined by the power-law between $N(L)$ and L (Mandelbrot 1967, 1983). This method has been applied to analyze two-dimensional projections of a particle and has two variants. The second, *correlation function method*, is to determine fractal dimension by exploring the dependence on distance r of the correlation function defined as $c(r) = \langle \rho(x)\rho(x+r) \rangle \propto r^{-\eta}$ where $\langle . \rangle$ denotes the spatial average; $\rho(x)$ is the density at a position x of a certain quantity. Fractal dimension can be determined by a simple relation $\beta = E - \eta$ where E is the Euclidean dimension of the space in which the aggregate is embedded (Forrest and Witten, 1979). The two methods examine a single particle with changing scales. The third method, *fractal measure method*, is to determine the fractal dimension by measuring properties of an ensemble of particles with similar shapes with the same scale (Sreenivasan, 1991). This method has a variety of variants based on different measures used. Typical examples are Mandelbrot's area-perimeter power-law and Mandelbrot's volume-area power-law (Mandelbrot, 1983, ch.12). The three major methods and their various variants are summarized in Table 1. Table 2a is a summary of area fractal dimensions. Table 2b is a summary of mass-fractal dimensions. The terms "mass fractal dimension and area fractal dimension" are used in this paper generically to connote, respectively, fractal dimensions of objects embedded in three-dimensional and two-dimensional Euclidean space. As shown in Table 2b fractal measure methods based on power-laws among different equivalent diameters and / or dynamic shape factors are commonly used for studying non-spherical aerosols.

Table 1. A Summary of Three Major Methods and Their Variants to Obtain Fractal Dimensions

Methods	Symbols	Power-law used	Description
Ruler Method	RM1	$P \propto L^{1-\beta_1}$	Fractal dimension β_1 is obtained by measuring boundary perimeter P with length-varying steps.
Ruler Method 2	RM2	$A \propto L^{\beta_2}$	Fractal dimension β_2 is obtained by measuring projected area A with length-varying squares for a particle
correlation function method	CF	$C(r) \propto r^{E-\beta_{cf}}$	Fractal dimension β_{cf} is obtained by measuring $c(r)$ variation with size r for a particle
Fractal measure method	FM	$q_i \propto q_j^{\beta_{ij}}$	Fractal dimensions are obtained by measuring (q_i, q_j) for an ensemble particles with similar geometry.
	FM1		$q_i = D_{me}, q_j = D_{ve}$
	FM2		$q_i = D_{ae}, q_j = M$
	FM3		$q_i = D_{ae}, q_j = D_{ae}$
	FM4		$q_i = \chi, q_j = D_{ve}$

D_{ve}, D_{ae} , and D_{me} are respectively volume, dynamical, and mobility equivalent diameters; χ is the dynamic shape factor; see Part I for their definitions.

2. Studies of Non-spherical Hydrometeors

Meteorologists treat non-spherical crystals in a way different from aerosol scientists. First, meteorologists prefer directly establishing relations between physical quantities (e.g., mass) for different hydrometeors to using some equivalent diameters and shape factors. Second, fractal geometry has found few explicit applications in hydrometeor shape characterization. However, fractal properties of hydrometeors have been implied, long before the birth of fractal geometry, in a large number of empirically power-laws. Various power laws, with integer or fractional exponents, are mathematical manifestations of physical objects as described by fractal geometry (Schroder, 1991). In fact, most fractal measure methods for aerosol particles can be related to these empirical power laws through the generalized power laws given in Part I. Since 1935, various power laws have been established for hydrometeors. A summary of them is desirable for linking hydrometeors with fractal geometry.

The most extensive power-laws for hydrometeors are established for mass: $M = \alpha_{MD} D^{\beta_{MD}}$. In 1935, Nakaya and Terada obtained mass power laws for five rough categories of hydrometeors: graupels, crystals with water droplets, powder snow and spatial dendrite crystals, plane dendrite crystals, and needles. Since then mass power-laws have been dramatically supplemented (Bashkirova and Pershina, 1964; Zikmunda and Vali, 1972; Locatelli and Hobbs, 1974; You et al., 1987; Mitchell et al., 1990). A summary is given in Table 3 after Locatelli and Hobbs (1974) and Mitchell et al. (1990).

Relatively small number of area (A) data have been published (Davis and Auer, 1974; Brintjies et al., 1987; Heymsfield and Kajikawa, 1987); but the number has been increasing recognizing the importance of area in both microphysics and radiation transfer (Mitchell and Arnott, 1994), and the development of instruments which can automatically sample and analyze two-dimensional images such as PMS-2D probes. Recently, the power-law for

Table 2a. Reported Values of the Fractal Dimensions of Two-Dimensional Projections

Particle type	β_a	Methods	Notes	Source
Fe, Zn, SiO ₂ , Lab	1.7 to 1.9	RM2 & CF	D: 1.1 to 3.0 μm D ₀ : 7nm	Forrest & Witten 1979
Acetylene soot, Lab	1.5 to 1.6	RM	D < 1.0 μm D ₀ : 30 nm,	Samson et al. 1987
Acetylene soot, Lab	1.82	RM	D: 5.5 to 12 μm D ₀ : 30 nm,	Samson et al. 1987
Methane soot, Lab	1.72 \pm 0.10	RM	D: 1 to 5 μm D ₀ : 20 nm,	Zhang et al. 1988
Diesel soot, Lab	1.12 to 1.2	RM1	D: 0.79 μm D ₀ : 50 to 100 nm	Klingen & Roth 1989
Carbonaceous aerosol	1.35 to 1.89	RM2	D: 0.21 to 2.61 μm D ₀ : 28 \pm 11 nm	Katrinak et al. 1993
soot	1.70 \pm 0.07	RM2		Cai et al. 1993
soot	1.57 \pm 0.08	CF		Cai et al. 1993

Table 2b. Reported Values of Mass-Fractal Dimensions

Particle type	β	Methods	Notes	Source
Ag aggregates	2.18	FM	D ₀ :7.5 nm	Schmidt-Ott 1988a
Ag aggregates	2.18	FM	D ₀ : 7.5 nm	Schmidt-Ott 1988a
Methane soot	1.62 ± 0.06	FM.	D: 1 to 5 μm D ₀ : 20 nm,	Zhang et al. 1988
Butane soot	1.9	FM	D < 20 μm D ₀ :60 nm,	Colbeck et al. 1989
PtO ₂	1.8 ± 0.05	FM	D ₀ :17 nm,	Naumann & Bunz 1991
U ₃ O ₈	1.8 ± 0.07	FM	D ₀ :36 nm,	Naumann & Bunz 1991
CuO	1.8 ± 0.05	FM	D ₀ :24 nm,	Naumann & Bunz 1991
UO ₂	1.9 ± 0.08	FM	D ₀ :46 nm,	Naumann & Bunz 1991
Fe ₂ O ₃	2.7 ± 0.04	FM	D ₀ :45 nm,	Naumann & Bunz 1991
Fe ₂ O ₃	2.7 ± 0.05	FM	D ₀ :45 nm,	Naumann & Bunz 1991
Carbonaceous aerosol	1.96	FM	D _{ve} :0.56 to 1.41	Wu & Colbeck 1991
soot	1.71 ± 0.10	RM2,3D		Cai et al. 1993
soot	1.57 ± 0.08	CF,3D		Cai et al. 1993
soot	1.93 ± 0.08	FM, h = 12 mm		Cai et al. 1993
soot	1.72 ± 0.07	FM, h = 16 mm		Cai et al. 1993
magnesium oxide smoke	1.08	FM	D _{ve} :0.63 to 1.58	Wu & Colbeck 1991
Butane soot	1.87 to 2.19	FM	D: ≤ 10 μm D ₀ :50 nm	Nyeki & Colbeck 1994

projected area of complex polycrystals in cirrus clouds was established. The projected area was measured for particles < 200 μm by photocopying replicator image under microscope. For sizes > 200 μm, the projected area was determined from the ice particle images of the 2D-C probe by counting the occluded pixels. Technique details are referred to Mitchell et al. (1996a, b). Table 4 is a summary of these power-laws.

Terminal velocity power-law $V_t = \alpha_v D^{\beta_v}$ results from the corporation of fractal geometry of a particle and fractal properties of flow around the particle (Part I). Empirical power laws have been reported since 1935 (Nakaya and Terada, 1935; Langleben, 1954 for plates

Table 3. Power-Laws between Mass and Maximum Diameter of Hydrometeor

Hydrometeor Type	Power-law	Notes	Authors
Lump graupel	$M = 0.042D^{3.0}$	D:0.5 to 2.0 ρ :0.05 to 0.1	L & H(1974)
Lump graupel	$M = 0.078D^{2.8}$	D:0.5 to 3.0 ρ :0.1 to 0.2	L & H(1974)
Lump graupel	$M = 0.14D^{2.7}$	D:0.5 to 1.0 ρ :0.2 to 0.45	L & H(1974)
Conical graupel	$M = 0.073D^{2.6}$	D:0.8 to 3.0	L & H(1974)
Hexagonal graupel	$M = 0.044D^{2.9}$	D:0.8 to 3.2	L & H(1974)
Graupellike snow of lump type	$M = 0.059D^{2.1}$	D:0.5 to 2.2	L & H(1974)
Graupellike snow of hexagonal type	$M = 0.021D^{2.4}$	D:0.8 to 2.8	L & H(1974)
Rimed columns	$M = 0.033D^{2.3}$	D:0.8 to 2.0	L & H(1974)
Rimed dendrites	$M = 0.015D^{2.3}$	D:1.8 to 4.0	L & H(1974)
Rimed radiating assemblages of dendrites	$M = 0.039D^{2.1}$	D:1.8 to 2.8	L & H(1974)
Aggregates of radiating assemblages of dendrites or dendrites	$M = 0.073D^{1.4}$	D:2.0 to 10.0	L & H(1974)
Aggregates of rimed radiating assemblages of dendrites or dendrites	$M = 0.037D^{1.9}$	D:2.0 to 12.0	L & H(1974)
Aggregates of side planes	$M = 0.047D^{1.4}$	D:0.5 to 4.0	L & H(1974)
Elementary needles	$M = 0.0049D^{1.8}$	D:0.6 to 2.7	M(1990)
Rimed Elementary needles	$M = 0.0060D^{2.1}$	D:0.5 to 2.8	M(1990)
Long columns	$M = 0.0121D^{1.8}$	D:0.2 to 1.5	M(1990)
combinations of Long columns	$M = 0.017D^{1.8}$	D:0.2 to 2.6	M(1990)
side planes	$M = 0.021D^{2.3}$	D:0.3 to 2.5	M(1990)
Short Columns	$M = 0.064D^{2.6}$	D:0.2 to 0.6	M(1990)
Combinations of short columns	$M = 0.031D^{1.9}$	D:0.4 to 1.4	M(1990)
Hexagonal plates	$M = 0.028D^{2.5}$	D:0.2 to 1.0	M(1990)
Radiating Assemblage plates	$M = 0.019D^{2.1}$	D:0.2 to 3.0	M(1990)
Fragments of rimed dendrites	$M = 0.027D^{1.7}$	D:0.3 to 1.9	M(1990)
Aggregates of fragments of rimed dendrites	$M = 0.034D^{2.0}$	D:0.5 to 4.8	M(1990)
Aggregates of radiating assemblages plates	$M = 0.023D^{1.8}$	D:0.8 to 7.7	M(1990)
Aggregates of side planes, bullets, and columns	$M = 0.022D^{2.1}$	D:0.8 to 4.5	M(1990)

L & H = Locatelli and Hobbs (1974); M = Mitchell et al. (1990)

Table 4. Area Power-Laws of Hydrometeors

Hydrometeor Type	Power-laws	Notes	Sources
Crystal with sector-like branches	$A = 0.65D^2$	10 to 40, basal	Davis and Auer1974
Crystal with sector-like branches	$A = 0.55D^{1.97}$	41 to 2000, basal	Davis and Auer1974
crystal with broad braches likerabbit ears, steller crystals	$A = 0.65D^2$	10 to 90, basal	Davis and Auer1974
crystal with broad braches like rabbit ears, steller crystals	$A = 0.11D^{1.63}$	91 to 1500, basal	Davis and Auer1974
crystal with broad sector-like braches	$A = 0.65D^2$	10 to 100, basal	Davis and Auer1974
crystal with broad sector-likebraches	$A = 0.21D^{1.76}$	101 to 1000, basal	Davis and Auer1974
solid thick plate	$A = 0.65D^2$	10 to 1000, basal	Davis and Auer1974
Solid column, $L / W \leq 2$	$A = 0.65D^2$	10 to 1000, basal	Davis and Auer1974
Solid column, $L / W > 2$	$A = 0.65D^2$	10 to 1000, basal	Davis and Auer1974
Hollow column, $L / W \leq 2$	$A = 0.65D^2$	10 to 1000, basal	Davis and Auer1974
Hollow column, $L / W > 2$	$A = 0.65D^2$	10 to 1000, basal	Davis and Auer1974
Hexagonal plates	$A = 0.65D^2$	10 to 3000, basal	Davis and Auer1974
Double plate with branches	$A = 0.72D^{1.7}$	$D > 200 \mu\text{m}$, basal	Bruitjes et al. 1987
Hexagonal plates	$A = 0.2395D^{1.855}$	$D > 15 \mu\text{m}$, random	Mitchell et al 1996
Hexagonal column	$A = 0.6837D^{2.000}$	$15 < D < 100 \mu\text{m}$	Mitchell et al 1996
Hexagonal column	$A = 0.04590D^{1.415}$	$D > 100 \mu\text{m}$	Mitchell et al 1996
Bullet rosettes with 5 branches	$A = 0.08687D^{1.568}$	$D > 200 \mu\text{m}$	Mitchell et al 1996
Complex Polycrystals	$A = 0.2285D^{1.88}$	$20 < D < 450 \mu\text{m}$	Mitchell et al 1996
Simple polycrystals	$A = 0.4715D^{2.0}$	$20 < D < 100 \mu\text{m}$	Mitchell et al 1996

and columns, dendrites, mixture of dendrites and aggregates of plates, rimed dendrites; Mason and Huggins, 1980 for hailstones; Sasyo and Matsuo, 1980 for mixed snowflakes; Locatelli and Hobbs, 1974 for 15 types of hydrometeors; Knight and Heymsfield, 1983 for hailstones; Heymsfield and Kajikawa, 1987). A summary is given in Table 5. Berry (1989) offered a good discussion on terminal velocity of aerosol particles.

The size of a crystal is usually be characterized by two lengths: length along a -axis (a) and length along c -axis (c). Observations (Schaefer, 1947; Wieckmann, 1947; Reynolds, 1952; Mason, 1953; Magono, 1954; Isono, 1959; Ono, 1969, 1970; Auer and Veal, 1970; Heymsfield and Knollenberg, 1972; Davis, 1974; Jayaweera and Ontake, 1974) have shown that the two

Table 5. Power-Laws between Different Characteristic Lengths of Hydrometeors

Hydrometeor type	Power-laws	Range of major axis (μm)	Sources
Hexagonal plate. E	$H = 1.41 \times 10^{-2} D^{0.474}$	10 to 3000	Auer and Veal(1970)
Crystal with sector-like branches. D	$H = 1.05 \times 10^{-2} D^{0.423}$	10 to 2000	Auer and Veal(1970)
crystal with broad braches like rabbit ears, steller crystals. B	$H = 9.96 \times 10^{-3} D^{0.415}$	10 to 1500	Auer and Veal(1970)
crystal with broad sector-like braches. C	$H = 9.96 \times 10^{-3} D^{0.415}$	10 to 1000	Auer and Veal(1970)
solid thick plate. F	$H = 0.138 D^{0.778}$	10 to 1000	Auer and Veal(1970)
Solid column, $L / W \leq 2$.G	$W = 0.578 L^{0.958}$	10 to 1000	Auer and Veal(1970)
Solid column, $L / W > 2$.I	$W = 0.260 L^{0.927}$	10 to 1000	Auer and Veal(1970)
Hollow column, $L / W \leq 2$.J	$W = 0.422 L^{0.892}$	10 to 1000	Auer and Veal(1970)
Hollow column, $L / W > 2$.H	$W = 0.263 L^{0.930}$	10 to 1000	Auer and Veal(1970)
dendrites, fernlike crystals, dendrites with plates at end, Plates with dendrite extensions, Four brached crystals, dendrites with 12 branches. A	$H = 9.02 \times 10^{-3} D^{0.377}$		Auer and Veal(1970)
Solid bullet, $L \leq 0.3$ mm. K	$W = 0.153 L^{0.786}$		Auer and Veal(1970)
Hollow bullet, $L \geq 0.3$ mm.M	$W = 0.063 L^{0.532}$		Jayaweera & Ontake 1974
Elementary needle. L	$W = 3.05 \times 10^{-2} L^{0.611}$		Heymfield 1972
Long solid column.N	$w = 3.53 \times 10^{-2} L^{0.437}$		Heymfield 1972

lengths are related to each other, and the size relationship can be well described by various power-laws. Table 6 is a summary after Pruppacher and Klett (1978, 40p). These power laws provide observational evidence for the existence of self-affine fractals, and hence necessitate the second order generalization of describing particle shapes.

III. FRACTAL DIMENSION, SELF-SIMILAR AND SELF-AFFINE FRACTAL

1. Fractal Dimension

Fractal dimension is the most important shape descriptor in fractal geometry. For completeness, this section outlines the evolution of dimension concept. The Euclidean dimension originates from intuition. We know empirically that the dimension of a line and a plane is 1 and 2, and that we live in a 3-dimensional space. Such intuitive dimension concept is generalized to n-dimensional vector space by defining the dimension of a vector space as the

number of independent variables (Datta, 1994). Actually, it is conventional in multi-body mechanics to replace the motion of m particles in 3 dimensions by the motion of one particle in $6m$ -dimensional space by considering each particle's location and momentum as independent. Poincare (1903) gave topological meanings to such intuitive view in terms of "continuum and cut". The following is the translation by Mandelbrot (1983, 410p): "If to divide a continuum C it suffices to consider as cuts a certain number of distinguishable elements, we say that this continuum is of dimension one.... If to divide a continuum it suffices to use cuts which form one or several continua of dimension 1, we say that C is a continuum of dimension 2. If cuts which form one or several continua of at most dimension two suffice, we say that C is a continuum of dimension three; and so on.... Since curves can be divided by cuts which are not continua, they are continua of dimension one; since surface can be divided by continuous cuts of dimension one, they are continua of dimension two; and finally space can be divided by a continuous cuts of two dimensions, it is a continuum of dimension three."

Table 6. Summary of Commonly-used Dimensions

Name	Description
Euclidean dimension	Dimension of the Euclidean space in which the observed set is embedded; integral values only
Topological dimension	Integral values only; invariant under homeomorphism
Similarity dimension	Defined for strictly self-similar objects, including Euclids
Hausdorff-Bestovish dimension	Defined by most efficient covering and for any shapes
Capacity dimension	Defined by covering with identical Euclids, e.g., spheres and cubes

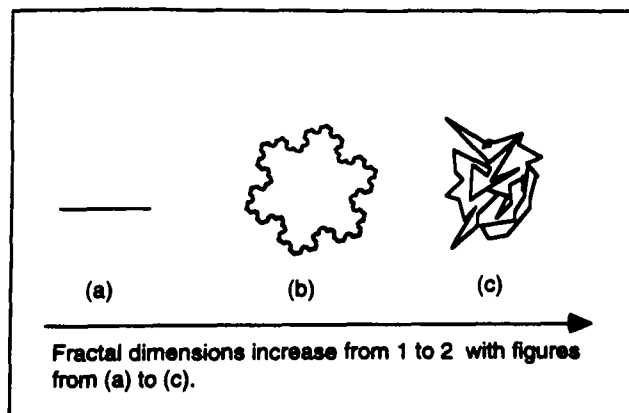


Fig.3. Objects with the same Euclidean dimension 1, yet different fractal dimensions, Object (a) is a smooth line with fractal dimension $\beta = 1.0$; object (b) is a Koch flake with fractal dimension $\beta \approx 1.26$; object (c) is a plane-filling Brownian motion curve with fractal dimension $\beta \approx 2$.

The dimension as discussed looks natural and is favored by common sense. It, however, contains serious flaws. First, it cannot differentiate between simple and complex shapes. For example, the objects in Fig.3 have the same Euclidean dimension 1, yet different shapes. Second, there are contradictions for complex shapes. For example, nearly one hundred years ago, Peano described a very strange curve that can be drawn with a single stroke and tends to completely cover a plane (Peano curve, see Mandelbrot, 1983). Since the location of a point on the Peano curve, like a point on any curve, can be characterized with one real number, we become able to describe the position of any point on a plane with only one real number. Hence both Euclidean and topological dimension of this curve are 1. This contradicts the empirical value 2 of a plane. These difficulties drove mathematicians to a concept breakthrough at the early 20th century: from topological notion to metric notion of dimension concept. These metric dimensions are called fractal dimensions by Mandelbrot (1983) (see Table 6 for a summary).

The simplest fractal dimension is similarity dimension. As discussed in Part I, it is developed for self-similar objects, and closely connected with our intuitive notion of Euclidean dimension. Some key points are repeated here.

A one-dimensional object, for example, a line segment, can be divided into N identical parts each of which is scaled down by the ratio $D_0 = \frac{D}{N}$ (D is length). A two-dimensional objects, such as a square, can be divided into N identical parts each of which is scaled down by a factor $D_0 = \frac{D}{\sqrt{N}}$. A three-dimensional object, like a solid cube, can be divided into N little cubes each of which is scaled down by a ratio $D_0 = \frac{D}{\sqrt[3]{N}}$.

To generalize, a β -dimensional self-similar object can be divided into N smaller parts each of which is scaled down by a factor

$$D_0 = \frac{D}{\sqrt[\beta]{N}}, \quad (1a)$$

or

$$N = \left(\frac{D}{D_0}\right)^\beta. \quad (1b)$$

The similarity dimension is given by

$$\beta = \frac{\log(N)}{\log\left(\frac{D}{D_0}\right)}. \quad (1c)$$

Similarity dimension overcomes the difficulties of the Euclidean dimension when an object is self-similar, and conforms to Euclidean dimension when an object is a Euclid (Mandelbrot, 1983).

A more general fractal dimension, Hausdorff-Bestovish dimension, was introduced by Hausdorff in 1919, completed by Bestovish and finally manipulated to study physical objects by Mandelbrot (1983). Hausdorff-Bestovish dimension is defined as follows by a method of coverings.

Let $\xi > 0$ and $\delta > 0$ be real numbers. Cover a set Ω by countable spheres whose diameters are all smaller than δ . Denoting the radii of the spheres by r_1, r_2, \dots, r_k , the ξ -dimensional Hausdorff measure is defined by

$$H^\xi(\Omega) \equiv \liminf_{\delta \rightarrow 0} \left(\sum_k r_k^\xi \right), \quad (2a)$$

where $\inf(\cdot)$ means the infimum.

For any given set Ω , this measure is proved to jump from zero to infinity at a critical value ξ , denoted by β_h . This critical value defined as Hausdorff–Bestovish dimension. Mathematically, we have,

$$\beta_h = \inf \left\{ \xi : H^\xi(\Omega) = 0 \right\} = \sup \left\{ \xi : H^\xi(\Omega) = \infty \right\}, \quad (2b)$$

$$\text{so that} \quad H^\xi(\Omega) = \begin{cases} \infty & \text{if } \xi < \beta_h \\ 0 & \text{if } \xi > \beta_h \end{cases} \quad (2c)$$

Hausdorff–Bestovish dimension equals to similarity dimension for self-similar fractals, and to Euclidean dimension for regular objects (Appendix A). The practical ruler method is developed from the covering idea.

2. Self-similar and Self-affine Fractals

Self-similar models enhance our ability of particle shape characterization by quantifying some irregular shapes. Nature, however, also produces neither Euclidean nor self-similar shapes. As a consequence, a unified treatment should be able to include more complex shapes. The self-affine model is obviously a good choice. A self-affine fractal is the natural generalization of a self-similar fractal. Their main distinction is that self-similar fractals scale isotropically (the same in all directions) whereas self-affine fractals scale anisotropically (differently in different directions). In other words, a self-affine fractal is directionally self-similar. Mathematically, a function is self-affine if it satisfies (3a)

$$f(\lambda_1 x_1, \lambda_2 x_2, \dots, \lambda_n x_n) \approx \lambda_1^{H_1} \lambda_2^{H_2} \dots \lambda_n^{H_n} f(x_1, x_2, \dots, x_n), \quad (3a)$$

where H_i is called the Hufst exponent; the symbol \approx means that (3a) holds statistically (Mandelbrot, 1983). When f is a function of one independent variable, equation (3a) reduces to a simple form:

$$f(\lambda x) \approx \lambda^H f(x). \quad (3b)$$

Equation (3b) expresses the fact that the function is invariant under the following scaling: enlarging along the x -axis by a factor of λ , followed by scaling the function value by a different factor λ^H . More about self-similarity and self-affinity are given in Appendix B.

However, the practical part of the generalization from self-similar to self-affine fractals is not as simple as the concept. Unlike self-similar fractals which have such nice properties that only a single fractal dimension is needed to quantify shapes, and that methods for determining fractal dimensions are well established, characterization of self-affine fractals still remains unsolved (Mandelbrot, 1985; Lovejoy and Schertzer, 1987). In the following section, we will demonstrate the self-affinity of atmospheric particles, and address problems involving their shape characterization.

IV. JUSTIFICATION FOR SELF-AFFINE PARTICLES

1. Power-laws between Lengths of Different Directions

An obvious feature of a self-affine fractal is that it scales differently in different directions. Suppose a fractal scales differently in the x and z direction (Lojevoy and Schertzer, 1987; Matsushita and Ouchi 1989):

$$L_x \propto \lambda^{H_x} \quad , \quad (4a)$$

$$L_z \propto \lambda^{H_z} \quad , \quad (4b)$$

where L_x and L_z are the lengths along x and z direction respectively, λ the scale factor, H_x and H_z the corresponding exponents.

A combination of (4a) and (4b) yields a power law between the two lengths:

$$L_z \propto L_x^{\beta_{zx}} \quad , \quad (5a)$$

$$\beta_{zx} = \frac{H_z}{H_x} \quad . \quad (5b)$$

Equation (5b) shows that the exponent β_{zx} does not equal 1 if an object is self-affine (scales differently in the x and z direction) and equals 1 if it is self-similar. For crystals x and z correspond to the a -axis and c -axis respectively. Therefore, self-similarity or self-affinity of crystals can be investigated by examining power laws between lengths of the a -axis and c -axis. Simple calculation of the exponents given in Table 5 yields a spectrum of β_{zx} , from 0.377 to 2.288. The degree of self-affinity of crystals becomes more evident in Fig. 4.

2. Dimensional Relation between Self-affine Fractals and Their Projections

Atmospheric particles exist in the three-dimensional space. However, most shape analyses are usually performed for their two-dimensional projections. A relationship between

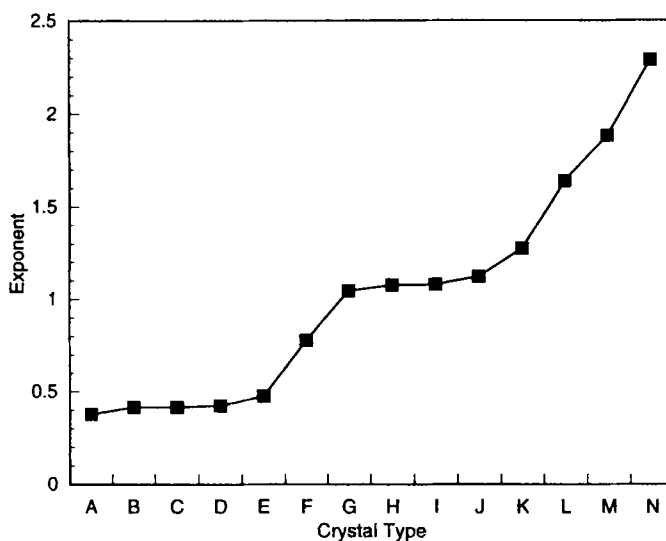


Fig. 4. Degree of Self-affinity of hydrometeors, the inverse of the exponents in Table 5 is taken wherever necessary.

mass and area fractal dimensions is therefore desirable. Two equations are in common use. First, for Euclidean particles, it is obvious that dimension of projections depends on both projected particles and projection subspace. A plane-projection of a three-dimensional and a two-dimensional particle has dimension two whereas a plane-projection of a one-dimensional curve still has dimension one. When a projection subspace is one-dimensional, either a three-dimensional, or a two-dimensional, or a one-dimensional object has a projection of dimension 1. This is readily generalized to a self-similar fractal (Part I):

$$\beta_{\text{projection}} = \min(\beta_s, \beta) . \quad (6a)$$

Equation (6a) indicates that the projection dimension $\beta_{\text{projection}}$ will be the minimum between β and β_s when a self-similar particle of dimension β is projected onto a subspace of dimension β_s . A rigorous demonstration of (6a) was provided in Falconer (1991, Ch.6).

The other method inferring mass fractal dimension from area-fractal dimension is based on Mandelbrot's rule of thumb for intersection (Mandelbrot, 1983). Mandelbrot's rule of thumb for intersections states that an E_s -dimensional section of a fractal set embedded in E -Euclidean dimensional space ($E > E_s$, integers) satisfies equation (7)

$$\beta = \beta_{\text{intersection}} + (E - E_s) \quad (6b)$$

Equation (6b) has been widely used for obtaining fractal dimension of an isotropic turbulence from its cross-sections, and adopted for cloud surface analysis assuming (6b) is valid for projections as well (see Malinowski and Zawadzki, 1993 and references therein).

However, when an object is self-affine, dimensional relationships are complicated. It will involve both (6a) and Mandelbrot's rule of thumb for intersections because of their anisotropic properties. For example, Malinowski and Zawadzki (1993) argued that satellite images of clouds are not cross-sections but rather horizontal projections. Particles exist in different orientations in the atmosphere; such orientational variability of atmospheric particles further compounds the problem. Assume that given an area-fractal dimension, the corresponding mass-fractal dimension lies between curves determined by (6a) and (6b). In other words, for self-affine particles, we can no longer predict mass-fractal dimension from area-fractal dimension from either (6a) or (6b). On the other hand, a combination of (6a) and (6b) sets the domain where mass-fractal dimensions locate. In practice, the common situation is that a particle embedded in the three-dimensional space is sampled onto a two-dimensional subspace, i.e., $\beta_s = E_s = 2$, and $E = 3$. Then (6a) and (6b) become (7a) and (7b) respectively.

$$\beta_2 = \min(2, \beta) , \quad (7a)$$

$$\beta = \beta_2 + 1 , \quad (7b)$$

where β_2 is the measured area-fractal dimension representing either $\beta_{\text{projection}}$ or $\beta_{\text{intersection}}$.

If our new proposal holds, then inferring mass-fractal dimension from area fractal dimension has a uncertainty of as large as 1. Knowledge of both mass fractal dimension and area fractal dimension is required to demonstrate (7a) and (7b). Unfortunately, to the authors' knowledge, very few studies have been performed which measure mass- and area-fractal dimensions simultaneously. Mitchell et al. (1996) provided 19 pairs based on previous studies for hydrometeors; Rogak et al. (1993) determined 12 pairs for aerosols. We plot these data in Fig.5. It is evident that the measurements fall within the domain set by (7a) and (7b). The preliminary agreement supports our assumption and suggests the existence of self-affine particles in the atmosphere. It also cautions that special care is needed to infer mass fractal dimension from area fractal dimension.

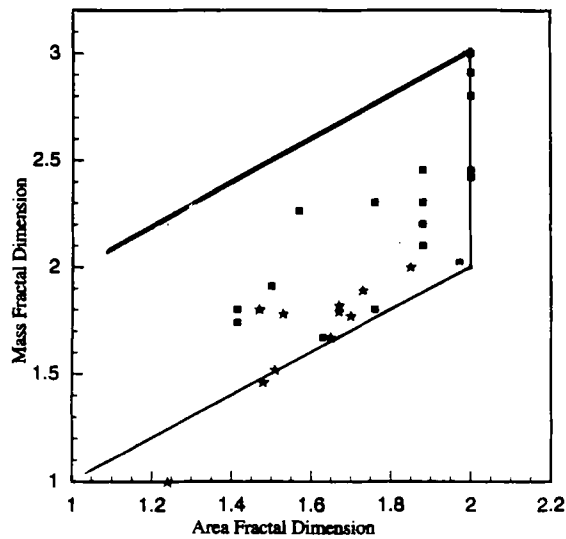


Fig.5. Relationship between mass fractal dimension and area fractal dimension. The squares represent the data for crystals from Table 1 of Michell (1994), and crosses represent the data for aerosol particles from Table 2 of Rogak and Flagan (1993). The thin solid curve represents $\beta_a = \min(2, \beta_m)$; the thick line represents $\beta_m = \beta_a + 1$.

V. IMPLICATIONS FOR SHAPE CLASSIFICATION AND INSTRUMENTATION

A variety of particle shapes exist in the atmosphere. Dependence of various properties (e.g., scattering and dynamical) on particle shapes makes particle shape classification more important. The traditional way to describe the shape is to use a metaphor or to compare the shape to a known geometry. For example, the British Standards Institute prepared a standard glossary of terms in the description of fine particle shapes (Kaye 1980, 338p). The most widely-used systematic classification of ice particles is that by Magono and Lee (1966), in which about 80 categories are identified. Obviously, these qualitative classifications hardly meet the needs of quantitative calculation such as numerical models.

Fractal theory offers a way to quantitatively classify particle shapes. However, practical application needs further examination. First, above discussions demonstrate that atmospheric particles can be characterized by a power-law:

$$(\text{quantity})_j = \text{prefactor}(\text{quantity})_i^{\text{exponent}} \quad (8)$$

The exponent, which is related to fractal dimension, is an important shape descriptor. For example, mass-fractal dimensions of atmospheric particles may range from 1 (needle crystals or straight chainlike aerosols), to 2 (regular planar crystals and aerosols), further to 3 (Euclidean 3-dimensional solid such as spherical particles), with various fractional dimensions in between. So far, most aerosol studies have emphasized the importance of fractal dimension; Information on prefactors has been overlooked. However, as pointed out by Mandelbrot, the prefactor cannot be neglected; it includes important information on particle texture. Furthermore, for atmospheric particles, the prefactor contains information about not only the common texture (characterized by a new term, lacunarity, defined by Mandelbrot, 1983) but also the particle material. Without knowing fractal geometry, meteorologists have reported a large number of empirical power laws. The importance of prefactor in character-

izing particle shapes can be clearly seen from these empirical power-laws. For example, in Table 3, hydrometeors of graupelike snow of lump type, rimed radiating assemblages of dendrites, rimed elementary needles, radiating assemblaged plates, and aggregates of side planes, bullets and columns, all have exponents around 2.1 whereas their shape differences are reflected by the differences in their prefactors. This suggests that exponent and prefactor should be measured and studied simultaneously as the first and second shape descriptor respectively.

Our second concern is for self-affine particles. As discussed above, we cannot definitely know mass-fractal dimensions from measuring two-dimensional images for self-affine particles. Quantifying self-affine particles requires at least a pair of power-laws that describe three physical properties. The existence of self-affine particles therefore calls for instruments which can measure both mass-and area-fractal dimensions together with prefactors. Developing such kind of instruments lies in the front of understanding atmospheric particle systems and their various effects. Recall Table 2 of Part I. determining terminal velocity or other dynamical quantities at least requires mass, area and maximum diameter. An optical example is that the determination of effective distance, the representative distance a photon travels through a particle, also requires mass, area and maximum diameter (Mitchell et al., 1996). Efforts have been recently made in this respect. Maloney et al. (1995) developed an instrument to measure solid particle length, width, cross-sectional area, external surface area and volume by rotating particles using a set of directed gas jets and recording image data for successive video fields as a function of rotation angle. Arnott et al. (1995) proposed a method to measure two-dimensional images and masses of cloud particles by recording successive images and the evaporation time.

VI. CONCLUDING REMARKS

Methods for studying non-spherical particles are reviewed. Examination is made of the differences in methods for aerosols and for hydrometeors. Various fractal dimensions and practical methods to determine them are discussed. Characterization of aerosol particles in terms of fractal dimensions is reviewed. Empirical power-laws for hydrometeors are summarized and re-considered in terms of fractal. It is argued that methods for aerosols and hydrometeors can be unified in terms of fractal through the generalized power laws as discussed in Part I.

Generalization from self-similar to self-affine particles is addressed. The degree of self-affinity of atmospheric particles is studied by examining power laws between lengths of different directions. It is shown that hydrometeors exhibit a spectrum of self-affinity, from self-similar to flat. It is further argued that unlike Euclidean or self-similar particles, self-affine particles have no definite dimensional relationship between real particles and their projections. We propose that the relationship for projections of self-similar particles and Mandelbrot rule of thumb for intersections respectively set the lower and upper limit to the mass-fractal dimensions given measured area-fractal dimensions. The preliminary evidence supports such relationship. Discussed is potential usefulness of power-laws in quantifying particle shapes. Exponent (or, fractal dimension) and prefactor in a power-law are suggested to be respectively the first and second index of a particle shape. Instruments are highlighted that can simultaneously measure both mass fractal dimension and area fractal dimension because of the existence of self-affine particle in the atmosphere.

Appendix A. Generality of Hausdorff–Bestovish Dimension

Falconer (1990, 29p) gave mathematical discussions about generality of Hausdorff–Bestovish dimension as follows.

If a set is smooth m -dimensional surface of space E^n then Hausdorff–Bestovish dimension equals m . In particular smooth curves have Hausdorff–Bestovish dimension 1 and smooth crves have Hausdorff–Bestovish dimension 2. For example, let F be a flat disc of unit radius in E^3 . From familiar properties of length, area and volume, their Hausdorff measures are

$$H^1(F) = \text{length}(F) = \infty, \quad (\text{A1.1a})$$

$$0 < H^2(F) = \frac{1}{4} \pi \text{area}(F) < \infty, \quad (\text{A1.1b})$$

$$H^3(F) = \frac{4}{3} \pi \text{volume}(F) = 0. \quad (\text{A1.1c})$$

Thus, According to Eq.2, Hausdorff–Bestovish dimension $\beta_h = 2$, equals the Euclidean dimension of the disc.

Appendix B. Self–similarity and Self–affinity

This appendix is after Mandelbrot (1983, Ch.39).

B1. Self–similarity

In the Euclidean space R^E ; a real ration $r > 0$ determines a transformation called similarity. It transforms the point $x = (x_1, x_2, \dots, x_E)$ into the point $r(x) = (r \times 1, r \times 2, \dots, r \times E)$, and hence transforms a set S into the set $r(S)$. A bounded set S is self–similar, with respect to r and an integer N , when S is the union of N non–overlapping subsets, each of which is congruent to $r(S)$. “Congruent” means identical except for displacement and or rotation.

B2. Self–affinity

In the Euclidean space R^E , a collection of positive ratios $r = (r_1, r_2, \dots, r_E)$ determines an affinity. It transforms each point $x = (x_1, x_2, \dots, x_E)$ into the point $r(x) = (r_1 \times 1, r_2 \times 2, \dots, r_E \times E)$, hence transforms a set into the set $r(S)$. A bounded set S is self–affine, with respect to the ratio vector r and an integer N , when S is the union of N nonoverlapping subsets, each of which is congruent to $r(S)$.

Appendix C. Corrections to Part I

Page 425, Table 2. $\chi = \rho_p \left(\frac{D_{ve}}{D_{ae}} \right)^{3b-1/b}$, not $\chi = \rho_p \left(\frac{D_{ve}}{D_{st}} \right)^{3b-1/b}$.

Page 430. Equation (14b) should be $\varepsilon_x = \frac{N}{X}$, instead of $\varepsilon_x = \frac{X}{N}$. Correspondingly, the following line “where ε_x represents the average X per particle” is changed as “where ε_x represents number of particles per unit X .”

Page 435. equation (A1) should be

$$L(\rho(x), q_1, q_2) = - \int_0^{\infty} \rho(x) \ln \rho(x) + \dots, \text{ not}$$

$$L(\rho(x), q_1, q_2) = - \int_0^{\infty} \rho(x) \ln(x) + \dots$$

The main idea took shape when Liu Yangang was in the Chinese Academy of Meteorological Sciences, PRC (CAMS) under the support of National Natural Science Foundation. Special thanks to Professors You Laiguang, Hu Zhijin, Guo Enming and Chen Wankui in CAMS. Liu Yangang thanks Drs. W. P. Arnott, D. L. Mitchell, J. Hallett and S. K. Chai of the Desert Research Institute, USA for their insightful discussions, thanks Mrs. Sharon Hughes of the Nevada Literacy Counsel, USA for her effort at improving English.

REFERENCES

- Arnott, W. P., et al. (1995), Direct airborne sampling of small ice crystals and the concentration and phase of haze particles, 9th symp. on Met, Observ, & Instr., 415-418.
- Auer, A., and D. Veal (1970), The dimensions of ice crystals in natural clouds, *J. Atmos. Sci.*, **27**: 919-926.
- Baron, P. A. and K. Willeke (1993), Aerosol fundamentals, In *Aerosol Measurement, Principles, Techniques and Applications*. (Eds) K. Willeke and Baron, 8-22 pp.
- Bashkirova, G., and T. Pershina (1964), On the mass of snow crystals and their fall velocities, *Tr. Gl. Geofiz. Observ.*, **165**: 83-100.
- Berry, M. V. (1989), Falling fractal flakes, *Physica D* **38**, 29-31.
- Bruintjies, R. et al. (1987), An examination of double-plate ice crystals and the initiation of precipitation in continental cumulus clouds, *J. Atmos. Sci.*, **44**: 1331-1349.
- Cai, J. et al. (1993), Comparison of size and morphology of soot aggregates as determined by light scattering and electron microscope analysis, *Langmuir*, **9**: 2861-2867.
- Colbeck, L. et al. (1989), The dynamics and structure of smoke aerosols, *J. Aerosol Sci.*, **20**: 875-878.
- Davis, C. L. and A. H. Auer (1974), Use of isolated orographic clouds to estimate the accuracy of diffusional ice growth equations, Proc. Cloud Phys. Conf. 1974, Tucson, USA, 141-147.
- Family, F. and T. Vicsek (1991), *Dynamics of Fractal Surfaces*, World Scientific, 480 pp.
- Falconer, K. (1990), *Fractal geometry: mathematical foundations and applications*, John Wiley & Sons, Chichester.
- Forrest, S. R. and Witten (1979), Long-range correlations in smoke-particle aggregates, *J. Phys. A12*, L109-L117.
- Herdan, G. et al. (1960), *Small Particle Statistics*, Butterworths, London.
- Heymsfield, A. J. (1972), Ice crystal terminal velocities, *J. Atmos. Sci.*, **29**: 1348-1357.
- Heymsfield, A. J. and M. Kajikawa (1987), An improved approach to calculating terminal velocities of plate-like crystals and graupel, *J. Atmos. Sci.*, **44**: 1088-1099.
- Kajikawa, M., and A. J. Heymsfield (1989), Aggregation of ice crystals in cirrus, *J. Atmos. Sci.*, **46**: 3108-3121.
- Katrinak, K. A. et al. (1993), Fractal geometry of carbonaceous aggregates from urban aerosol, *Environ. Sci. Technol.*, **27**: 539-547.
- Kaye, B. H. (1978), Specification of the ruggedness and / or texture of a fine particle profile by its fractal dimension, *Powder Technol.*, **21**: 207-213.
- Kaye, B. H. (1981), *Direct Characterization of Finaparticles*, John Wiley & Sons, New York.
- Klingen, H. J. and P. Roth (1989), Size analysis and fractal dimension of diesel particles based on REM measurements with an automatic imaging system, *J. Aerosol Sci.*, **20**: 861-864.
- Knight, N. C., and A. J. Heymsfield (1983), Measurement and interpretation of hail density and terminal velocity, *J. Atmos. Sci.*, **40**: 1510-1516.
- Korvin, G. (1992), *Fractal Models in Earth Science*, Elsevier, Amsterdam.

- Langleben, M. P. (1954), The terminal velocity of snowflakes, *Q. J. Met. Soc.*, **80**: 174–184.
- Lesaffre, F. (1989), Characterization of aerosol aggregates through fractal parameters, Effects due to humidity, *J. Aerosol Sci.*, **20**: 857–860.
- Liu, Y. (1995), On the generalized theory of atmospheric particle systems, *Adv. Atmos. Sci.*, **12**: 419–438.
- Lovejoy, S. and D. Schertzer and A. A. Tsonis (1987), Functional box-counting and multiple elliptical dimensions in rain, *Science*, **235**: 1036–1038.
- Locatelli, J. D., and P. V. Hobbs (1974), Fall speeds and masses of solid precipitation particles, *J. Geophys. Res.* **79(15)**: 2185–2197.
- Magill, J. (1991), Fractal dimension and aerosol particle dynamics, *J. Aerosol Sci.*, **22**: S165–168.
- Magono, C., and C. W. Lee (1966), Meteorological classification of natural snow crystals, *J. Fac. Sci., Hokkaido Univ.*, Ser 7 II, 321–335.
- Malinowski, S. P. and L. Zawadzki (1993), On the surface of clouds, *J. Atmos. Sci.*, **50**: 5–13.
- Maloney, D. J. et al. (1995), A new approach to determine external surface and volume of irregularly shaped particles, *Aerosol Sci. and Technol.*, **22**: 60–72.
- Mandelbrot, B. B. (1967), How long is the coast of Britain? Statistical self-similarity and the fractal dimension, *Science*, **165**: 636–638.
- Mandelbrot, B. B. (1983), The fractal geometry of nature, W. H. Freeman and Company, New York.
- Mitchell, D. L. (1996), Use of mass- and area-dimensional power-laws for determining precipitation particle terminal velocities, *J. Atmos. Sci.*, **53**: 1710–1723.
- Mitchell, D. L. et al. (1990), Mass-dimensional relationships for ice particles and influence of riming on snowfall rates, *J. Appl. Meteor.*, **29**: 153–163.
- Mitchell, D. L. et al. (1996a), Modeling cirrus clouds, Part I: Treatment of bimodal size spectra and case study analysis, *J. Atmos. Sci.*, **53**: 2952–2966.
- Mitchell, D. L. et al. (1996b), Modeling cirrus clouds. Part II: Treatment of radiative properties, *J. Atmos. Sci.*, **53**: 2967–2988.
- Nakaya, U., and T. Terada (1935), Simultaneous observations of the mass, falling velocity and form of individual snow crystals, *J. Fac. Sci. Hokkaido Univ.*, Ser. II, 1, 191–201.
- Naumann, K. H. and H. Bunz (1991), Aerodynamic properties of fractal aerosol particles, *J. Aerosol Sci.*, **22**: S161–164.
- Nyeki, S. and Colbeck, I. (1994), The measurement of the fractal dimensions of individual in situ soot agglomerates using a modified Millikan cell technique, *J. Aerosol Sci.*, **25**: 75–90.
- Pruppacher, H. R., and J. D. Klett (1978), Microphysics of Clouds and Precipitation, *D. Reidel*.
- Rogak, S. N. and Flagan, R. C. (1993), The mobility and structure of aerosol agglomerates, *Aerosol Sci. and Technol.*, **18**: 25–47.
- Samson, R. J. et al. (1987), Structural analysis of soot agglomerates, *Langmuir*, **3**: 272–281.
- Sander, L. M. (1985), Growth by particle aggregation, in *Scaling Phenomena in Disordered System*, (Eds.) R. Pynn and A. Skjeltorp, 31–48 pp.
- Scheoeder, M. (1991), *Fractals, Chaos, Power Law*. W. H. Freeman and Company, New York.
- Schmidt-Ott, A. (1988a), In situ measurement of the fractal dimensionality of ultrafine aerosol particles, *Appl. Phys. Lett.*, **52**: 954–956.
- Schmidt-Ott, A. (1988b), New approaches to in situ characterization of ultrafine agglomerates, *J. Aerosol Sci.*, **19**: 553–563.
- Schmidt-Ott, A. et al. (1990), Scaling behaviour of physical parameters describing agglomerates, *J. Aerosol Sci.*, **21**: 711–717.
- Takayasu, H. (1990), *Fractals in the Physical Sciences*, John Wiley & Sons, Chichester.
- Tohno, S. and K. Takahashi (1990), Morphological and dynamic characterization of Pb fume particles undergoing Brownian coagulation, *J. Aerosol Sci.*, **21**: 719–732.

-
- Wu, Z. and Colbeck, I. (1991), Measurement of the dynamic shape factor of fractal clusters, *J. Aerosol Sci.*, **22**: S239-240.
- You, L., Y., Chen and T. Wang (1987), A study on the relationship between the masses and dimension of snow crystals, *J. Academy Meteor. Sci.*, **2**: 197-201.
- Zhang, H. X. et al. (1988), In situ optical structure factor measurements of an aggregating soot aerosol, *Langmuir*, **4**: 867-871.
- Zikmunda, J. and G. Vali (1972), Fall patterns and fall velocities of rimed ice crystals, *J. Atmos. Sci.*, **29**: 1334-1347.
- Zikmunda, J. (1972), Fall velocities of spatial crystals and aggregates, *J. Atmos. Sci.*, **29**: 1511-1515.